Excitable modes in forced symmetry breaking for a cylindrical container with one rotating endwall

Yiannis Ventikos

Computational Biothermofluidics and Dynamical Systems Group,
Laboratory of Thermodynamics in Emerging Technologies,
Swiss Federal Institute of Technology,
Sonneggstrasse 3, ETH-Zentrum, Zurich, CH-8092, Switzerland
e-mail: Yiannis.Ventikos@ethz.ch

ABSTRACT

The technical relevance of swirling flows has inspired numerous investigations into the field: swirling flow burners, trailing vortices of delta wings, separators etc. are some of the applications where such research has yielded interesting results. At the same time, geophysics-inspired general swirling flow studies provided much input to this field. A subcategory of swirling flows is that where vortex breakdown is observed. Vortex breakdown is a condition where a vortex core undergoes a transformation from a slender flow entity to a structure of a drastically different nature: in the literature, numerous manifestations of this phenomenon have been reported, along with classification proposals for the flow structures connected with vortex breakdown.

A particular class of vortex breakdown types, i.e. that of bubble breakdown, has attracted a significant portion of the attention of researchers in the field, for its technical relevance, but also for a reason that is of particular interest to this work: it has been shown that steady and unsteady bubble-type vortex breakdown can be produced in a almost ideally controllable environment, i.e. in a completely enclosed cylindrical container with one spinning endwall, figure 1, (or in more intricate variations of this system). Such a geometrical configuration enjoys the benefit of being described fully by 2 parameters, i.e. the Reynolds number (based on the container diameter and the angular velocity of the rotating lid) and the aspect ratio. Additionally, there are no arbitrary or difficultly controllable boundary conditions (inflow/outflow), since all boundaries are either stationary or spinning solid walls.

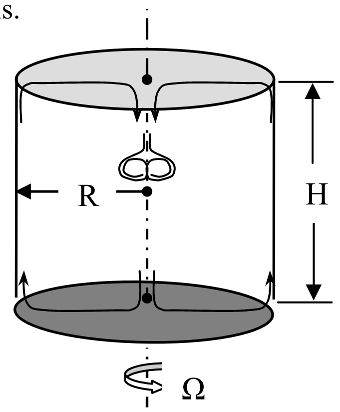

$$\mathbf{Re} = \frac{\mathbf{R^2 \Omega}}{\mathbf{\nu}}$$

$$a = \frac{H}{R}$$

Figure 1. Schematic configuration of the cylindrical container with one rotating endwall, location of vortex breakdown bubble of interest to this work and controlling parameters.

An additional strong motivating force favoring the investigation of flow configurations like the one described herewith has emerged recently: in microfluidic configurations, swirling flows are possibly the best candidates for achieving high mixing efficiencies: one of the principal reasons that microscale flow-based devices are very difficult to manufacture is that it is practically impossible to benefit from the intense mixing introduced by turbulent scales, because turbulence is non-existent at those small scales, [1].

The system under consideration has been particularly attractive to swirling flow investigators because strong experimental evidence supported the observation that for a particular range of the parameters, the flow seems to maintain the geometric symmetries of the confining geometry and forcing and thus presents us with axisymmetric conditions, [2]. Based on such observations, numerous computational investigations have been conducted, [3], [4], etc. that yielded excellent qualitative and quantitative comparisons with available experimental observations and measurements and moreover led to very interesting and novel insights on the system and its evolution as the parameters change.

Recently however, departures from this track have been reported: more specifically, in [5] an experimental investigation was conducted that showed both indications of vortex breakdown bubbles that were significantly more disorganized than the axisymmetric hypothesis allowed, and revealed sidewall flow structures that departed from a typical helical trajectory and involved patterns not explicable under the rotational symmetry assumption. This set of observations was further reinforced by computational investigations into the details of the breakdown bubbles: in [6] it was showed that the bubbles might not be the assumed closed recirculating entities that were believed to be, but that very rich dynamics were hidden in the subtle asymmetries that were *a posteriori* identified in all experimental visualizations but not paid due attention. Subsequently, [7] showed that the vortex breakdown bubbles can be objects exhibiting chaotic advection and that the origin of their anomalous behavior is the three-dimensionality originating at the side wall of the container. In [8] it was shown that the computational origin of the above mentioned phenomena can be attributed to perturbations imposed by the mesh topology. However, in the same work it was shown that the same non-axisymmetric and chaotic bubble behavior can be reproduced by other, more physically addressable types of perturbation, like minute distortions of the shape of the container. In the same work it was shown that the exact same numerics can produce axisymmetric bubbles under zero perturbation conditions. As a corollary it was argued that a perturbation-free environment is impossible in real experimental rigs, thus the forced symmetry breaking of perturbed containers (real and numerical) is the technically relevant case to look into. In a recent addition to the literature in the field, [9], it was shown numerically that even minute differences in the density between the working fluid and the agent utilized for visualization are adequate to lead to observations that carry non-axisymmetric features, even under the assumption of an underlying axisymmetric flow field.

Percentage → Type of disturbance ↓	0.0 %	0.1%	0.5%	1.0 %	2.0 %	5.0%
Oval x2 mode	G1, G2	G1, G2	G1,G2,G3	G2	G2	G2
Oval x4 mode				G2		
Top tilt		G1,G2	G2	G1	G2	G2
Eccentric rot.		G2	G2	G1,G2	G2	G2
Combination			G1,G2	G1,G2		
G I grid: 101 x 49 x 33		G II grid: 201 x 97 x 67			G III grid: 201 x 193 x 67	
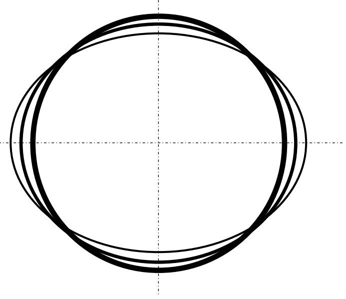		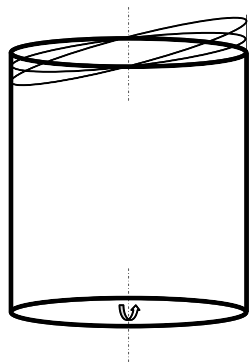			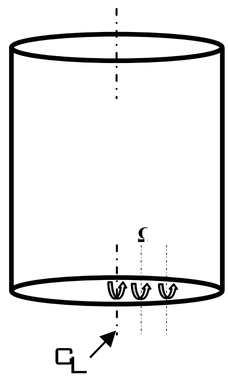	

Table 1. Summary of cases examined and grids utilized. The set of cases designated as “Combination” entails the co-existence of all 3 disturbances, in a randomly non-aligned manner.

We are reporting a small yet representative set of results examining the correlation between geometric imperfections of the container and observable departures from axisymmetric conditions. Our goal is to connect the subtle (or often not so subtle) non-axisymmetric features observed in all the available experimental results with possible underlying sources for the perturbations. Moreover, we are examining the perturbation kinetic energy distributions for various types of disturbances, thus identifying regions and modes that accumulation of energy is occurring in such forced symmetry breaking conditions.

A large number of spatially and temporally resolved simulations have been performed in order to understand the behavior of the system under investigation. An initially perfectly axisymmetric discretization that is distorted at modes and proportions that are characteristic of realistic imperfections present at experimental rigs constitutes the basis of this investigation. Table 1 describes sketchily the perturbations imposed, the runs conducted and the grids utilized. It has been shown, [8], that although Grid I of this Table is probably inadequate for the capturing of the perturbation quantities (in spite of the fact that it portrays the basic flow parameters accurately), Grids II & III yield practically identical results for all observables of interest. Although the computations were conducted in a time accurate manner, all simulations led eventually to fully stationary solutions. All the results reported here were computed using a second order accurate (in space and time) pressure correction method, based on the PISO approach, on a staggered grid, [10].

Results concerning the sidewall flow response to the distortion are shown in figure 2. Figure 2.a. shows iso-surfaces of radial perturbation velocity (one positive and one negative). The perturbation quantities have been computed either by referring both the distorted and ideally axisymmetric solutions to the ideally axisymmetric grid (thus making a small error due to the fact that the geometric locations of the distorted grid nodes differ slightly from those of the non-distorted grid), or by conducting a tri-cubic interpolation from the distorted field (grid and velocities) to the ideal grid and conducting the subtraction at the same node locations (introducing however the interpolation error). Both results were visually identical and we chose to report those of the second approach. Figure 2.b. shows the kinetic energy carried by the perturbation field. In spite of the fact that the distortion in the case presented was of mode x2, the kinetic energy of the disturbance presents us with 4 branches.

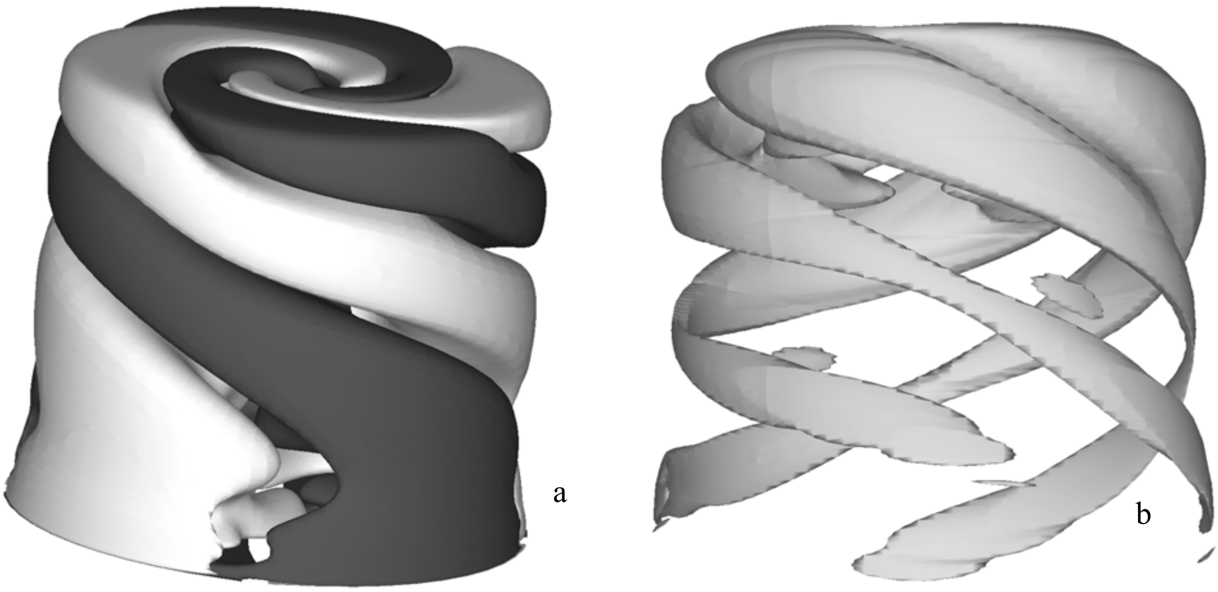

Figure 2.a. Positive and negative iso-surfaces for the radial perturbation velocity component, 1.0% of a mode x2 oval distortion. b. Iso-surface of the kinetic energy carried by the perturbation velocity field, for the same test case.

Figure 3.a. depicts the circumferentially averaged kinetic energy for the case of mode x2 oval 0.5% distortion, whereas figure 3.b. shows the same quantity for twice the distortion (1.0%). The relative magnitudes of the peak perturbation energies differ by more than 1 order of magnitude, an observation that underpins the sensitivity of the system to geometric imperfections. A similar trend was found for the rest of the cases of this type of distortion simulated, as well as for other types of container imperfection, where such observations could be conducted.

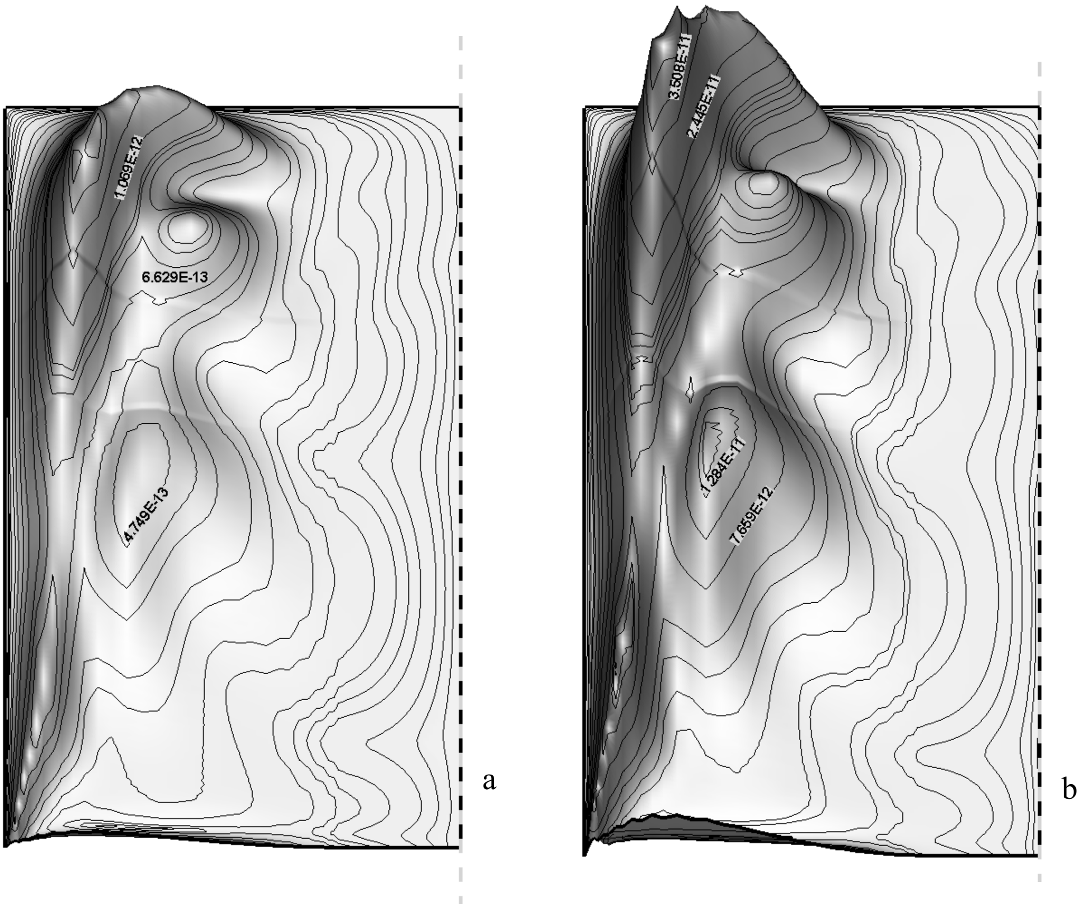

Figure 3.a. Depiction of the circumferentially averaged kinetic energy of the perturbation for a case of oval mode x2 disturbance of 0.5% magnitude. b. Same quantity for the oval mode x2 case of 1.0% distortion magnitude. Dashed line designates the axis of symmetry, rotating wall at bottom.

REFERENCES

[1] A. D. Stroock, S.K.W. Dertinger, A. Adjari, I. Mezić, H.A. Stone, G. M. Whitesides, "Chaotic mixer for microchannels", Science, 295,pp 647-651, 2002,

[2] M, M. P. Escudier, "Observations of the flow produced in a cylindrical container by a rotating endwall," Exp. Fluids 2 4, pp. 189-196, 1984

[3] J. M. Lopez. "Axisymmetric vortex breakdown: Part 1. Confined swirling flow", J. Fluid Mech. 221, pp. 533-552, 1990

[4] G. L. Brown, J. M. Lopez, "Axisymmetric vortex breakdown. Part 2: Physical mechanisms," J. Fluid Mech. 221, pp. 553-576, 1990

[5] A. Spohn, M. Mory, E. J. Hopfinger, "Experiments on vortex breakdown in a confined flow generated by a rotating disk," J. Fluid Mech. 370, pp. 73-99, 1998

[6] F. Sotiropoulos, Y. Ventikos, " The three-dimensional structure of confined swirling flows with vortex breakdown", J. Fluid Mech. 426, pp. 155 – 175, 2001

[7] F. Sotiropoulos, Y. Ventikos, T. C. Lackey, "Chaotic advection in 3-D stationary vortex-breakdown bubbles: Šil'nikov's chaos and the devil's staircase", J. Fluid Mech., 444, pp. 257-297, 2001

[8] Y. Ventikos, "The effect of imperfections on the emergence of three-dimensionality in stationary vortex breakdown bubbles", Phys. Fluids, 14(3), 13-16, 2002

[9] A. Yu. Gelfgat, "Three-dimensionality of trajectories of experimental tracers in a steady axisymmetric swirling flow: effect of density mismatch", Theoret. Comput. Fluid Dynamics, 16, pp 29-41, 2002

[10] Y. Ventikos, G. Tzabiras, "A numerical method for the simulation of steady and unsteady cavitating flows", Comput. Fluids 29(1), pp. 63-88, 2000